Adaptive Coverage Control with Power-Aware Control Laws and Exponential Forgetting

Mert Turanli, Hakan Temeltas

***Abstract*— In this paper, we extend the coverage control problem by using adaptive coordination with exponential forgetting and power aware control laws. The Centroidal Voronoi Tesellations enable the nonholonomic mobile nodes position themselves sub-optimally according to a time-varying density function. The Lyapunov stability analysis of the adaptive and decentralized approach is presented. The synchronization among the mobile nodes is achieved by using a linear consensus protocol. Also, repulsive forces prevent nodes from collision. Simulation results show that by using power aware control laws, energy consumption of the nodes can be reduced.**

I. Introduction

Multi agent coordination problems are challenging topics studied intensively in the past years. In many applications, using more than one agent is necessary to achieve better results. This is the case in multi agent coverage problem. Distributed coverage control topic has its importance in mobile sensor networks. It uses locational optimization to place the sensors in optimal way in order to improve coverage performance.

In literature, there are various examples of placing sensors in an environment using locational optimization. Luna *et. al* [1], propose an adaptive and decentralized version of coverage control approach which uses nonholonomic mobile sensors and time varying density functions. In [2], a distributed control law and coordination algorithm is proposed which uses location dependent sensing models. Another example [3] proposes an adaptive and distributed approach which uses gradient descent algorithms to ensure optimal coverage and sensing policies.

In [4], a Local Voronoi Decomposition algorithm is proposed which accomplishes a robust and online task allocation. The results of algorithm is verified in the problem of exploration of an unknown environment. Okabe *et. al* [5] investigates eight types of locational optimization problems that can be solved by using Voronoi diagrams. The solution of these problems may involve different types of Voronoi diagrams. Another work in [6] considers a mobile sensor network which is capable of self-deployment. A potential field based approach is proposed which enables the nodes to be repelled by other nodes and obstacles. In [7], distributed optimal control problems for interacting subsystems are solved by using a distributed horizon control implementation. The implementation is used in multi-vehicle formation stabilization.

Another approach is to use probabilistic models to achieve optimal configuration. In [8], anisotropic sensors are defined by a probabilistic model and distributed control algorithms are proposed which maximize joint detection probabilities. Another distributed coverage approach [9] uses mobile sensors with limited range defined by a probabilistic model. It also uses joint detection probabilities and communication cost is integrated into coverage control problem.

There are also some examples which take energy consumption into account. Gusrialdi *et al.* [10], present a standard distributed coverage control algorithm combined with leader-following algorithm which maintains optimal energy utilization. Kwok *et al.* [11] uses power-aware coverage algorithms to adjust the energy consumption over the sensor network with two modified Llyod-like algorithms. In [12], an approach for agents with limited power to move considering power constraints is presented. Several types of Locational Optimization Functions are used and objective functions take global energy and different coverage criteria into account. Another example [13] discusses an energy efficient deployment algorithm based on Voronoi diagrams. The performance of the proposed algorithm is tested in terms of different criteria.

There are several contributions of this paper to the literature. A power-aware control law is proposed which reduces the energy consumption of the nodes optimally. To the best of author's knowledge, this is the first work that uses adaptive coverage with power-aware control laws and exponential forgetting. Also, repulsive forces are used to prevent nodes from collision.

The paper is organized as follows: In Section II, mathematical background of the optimal coverage control problem is given. In Section III, the adaptive coverage control with integrator dynamics is mentioned. Section IV describes the application of the adaptive coverage control for nonholonomic sensors. In Section V, we present the energy consumption model and the power-aware adaptive coverage control laws. In Section VI, the Lyapunov stability analysis of the power-aware adaptive coverage control law is presented. Section VII presents the simulation results and the conclusions of the presented work are given in Section VIII.

II. Problem Formulation

In this section, preliminary information for adaptive coverage control problem is presented.

M. Turanli and H. Temeltas are with the Department of Control and Automation Engineering, Istanbul Technical University, Maslak, Istanbul, 34469 TURKEY (e-mail: {turanlim, hakan.temeltas}@itu.edu.tr).

A. Voronoi Tessellations

As given in [1], the set V_k is called Voronoi tessellation of open set $S \subseteq \mathbb{R}^N$ if $V_k \cap V_l = \emptyset$ for $k \neq l$ and $\bigcup_k V_k = S$. The Voronoi region V_k is defined by:

$$V_k = \{q \in S \mid \|q - p_k\| \leq \|q - p_l\|, k \neq l\} \quad (1)$$

The $\| \quad \|$ operator is defined as Euclidean norm in $\mathbb{R}^N$ and the points p_k are called as generator points.

Fortune's Sweepline algorithm is used for calculating Voronoi regions.

B. Optimal Coverage Formulation

Consider $S \subset \mathbb{R}^N$ as a bounded environment and $\phi: \mathbb{R}^N \to \mathbb{R}^+$ as a density function. Let $f: \mathbb{R}^+ \to \mathbb{R}$ be a non-increasing performance function. Then we define locational optimization function as follows:

$$\mathcal{H}(p_1, p_2, \dots, p_m) = \sum_{k=1}^{n} \int_{V_k} f(\|q - p_k\|)\phi(q)dq \quad (2)$$

The V_k is Voronoi region k and p_k is the generator point of the corresponding Voronoi cell and m is the number of the generator points.

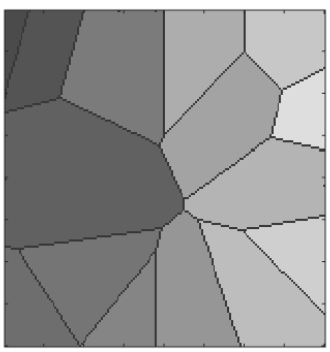

Figure 1. Example Voronoi Tessellation

The centroid C_{V_k} and mass M_{V_k} of Voronoi regions are defined in [3] are given by the following equations:

$$C_{V_k} = \frac{1}{M_{V_k}} \int_{V_k} q\phi(q)f(q)dq \quad (3)$$

$$M_{V_k} = \int_{V_k} \phi(q)f(q)dq \quad (4)$$

If we define the function $f(\|q - p_k\|) = \|q - p_k\|^2$ and take the partial derivative of locational optimization function $\mathcal{H}$ with respect to p_k, we get the following equations:

$$\mathcal{H} = \sum_{k=1}^{n} \int_{V_k} \frac{\partial f}{\partial p_k} \phi(q)dq \quad (5)$$

$$\frac{\partial \mathcal{H}}{\partial p_k} = \sum_{k=1}^{n} 2M_{V_k}(p_k - C_{V_k}) \quad (6)$$

In order to minimize the locational optimization function given in (2), the positions of the agents should be equal to the centroid positions calculated in (3). These types of diagrams are called as Centroidal Voronoi Tessellations.

Additionally, the density function $\phi(q)$ may change with respect to time or time-invariant. In the first case, $\phi(q, t)$ is called as time-varying distributed density function. If it is time-invariant, $\phi(q)$ is called as time-invariant distributed density function, as defined in [1].

III. Adaptive Coverage Control with Integrator Dynamics

In the integrator dynamics case, the agents are modeled as single integrators. The parameter vector $\varsigma \in S \to \mathbb{R}_+^m$ and vector function $\mathrm{Z} \in S \to \mathbb{R}_+^m$ are defined in [1] as follows:

$$\phi(q) = \mathrm{Z}^T(q)\varsigma \quad (7)$$

For each element of vector ς, the following condition should be also satisfied:

$$\varsigma(j) \geq \alpha, for\ j = 1, 2, \dots m \quad (8)$$

The lower bound of the vector ς prevents the distributed density function from taking zero values while calculating the centroids of the Voronoi regions.

The estimate of parameter vector and estimated value of the distributed density function and estimation error for k^{th} agent can be represented as:

$$\hat{\phi}_k(q) = \mathrm{Z}^T(q)\hat{\varsigma}_k \quad (9)$$

$$\tilde{\varsigma}_k = \hat{\varsigma}_k - \varsigma_k \quad (10)$$

An adaptive control law proposed in [1] is used to calculate estimated centroid locations and to drive the agents to an optimal configuration. Also, a linear consensus protocol is used in estimation to speed up the convergence of the parameter error vectors to zero.

IV. Adaptive Coverage Control for Team of Nonholonomic Agents

An adaptive control law with linear consensus for a nonholonomic agent model is proposed in this section.

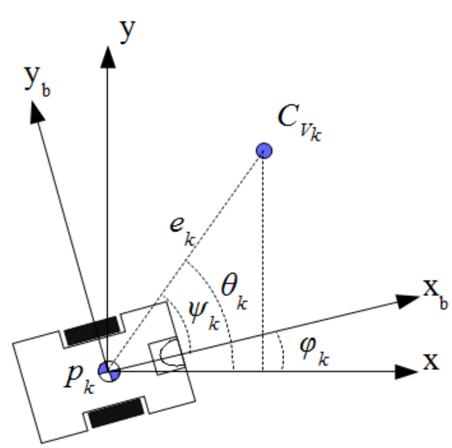

Figure 2. Position of the agent and model parameters

A. Control Law for Nonholonomic Agents

In this work, the control law used in [1] with a unicycle model proposed in [14] is used to drive the agents to the centroid locations.

$$\begin{pmatrix} \dot{e}_k \\ \dot{\psi}_k \\ \dot{\theta}_k \end{pmatrix} = \begin{pmatrix} u_k \, cos\psi_k \\ -\omega_k + u_k \frac{sin\psi_k}{e_k} \\ u_k \, \frac{sin\psi_k}{e_k} \end{pmatrix} \tag{11}$$

The control law proposed in [1] is:

$$\begin{pmatrix} u_k \\ \omega_k \end{pmatrix} = \begin{pmatrix} (\gamma cos\psi_k) e_k \\ 2\gamma sin\psi_k cos\psi_k + \lambda(\psi_k + \theta_k) \end{pmatrix} \tag{12}$$

In Figure 2, the position of the agent and the centroid location for a single agent is given as p_k and C_{V_k}. Here, u_k and ω_k are linear and angular control inputs, respectively. φ_k is the heading angle, e_k is the Euclidean distance between the agent and the centroid, ψ_k is the angle between the agent and the centroid.

Here, $\gamma > 0$ and $\lambda > 0$ are control gains. The control law drives the agents to the centroid C_{V_k} positions.

B. Nonholonomic Adaptive Coverage Control

The adaptation law proposed in [1] is used to estimate the parameters of the distributed density function:

$$e_1 = Z(\hat{\varsigma}_k - \varsigma_k) \tag{13}$$

$$\dot{\hat{\varsigma}}_k = -\mathrm{P}\mathrm{Z}^T e_1 - \eta \sum_{l \in \mathcal{L}_k} (\hat{\varsigma}_k - \hat{\varsigma}_l) \tag{14}$$

$$\dot{P}(t) = \lambda_f(t) P - P Z^T Z P \tag{15}$$

Here, $\lambda_f(t) > 0$ is the time-varying forgetting factor, $\eta > 0$ is the consensus gain, I is the identity matrix and Z denotes the vector function given in (7).

The first term in (14) is the least squares estimator with exponential forgetting [15] and the second term gives the consensus protocol [1]. The stability analysis of the adaptation rule will be given in the related section.

A linear consensus protocol is used in the estimation of the parameter vector for a single agent. In an undirected graph of the mobile agents and vertices $V_g = \{v_1, v_2, \dots, v_n\}$, the agents share their estimated parameter vector. Let the neighborhood of k^{th} agent be defined as:

$$\mathcal{L}_k = \{ l \mid \{v_k, v_l\} \in G \} \tag{16}$$

The communication among the nodes can be represented by the edges $G = \{g_1, g_2, \dots, g_m\}$ where j^{th} element of G is $g_j = \{v_k, v_l\}$. The consensus protocol speeds up the convergence of the estimation for the mobile agents.

V. Power-Aware Adaptive Coverage Control

In real applications, the mobile agents have limited energy storage. Thus, power aware control laws considering the energy consumption of the mobile agents are proposed in this section. The energy consumption model and control laws are given and in the third section, the repulsive forces are used for collision avoidance.

A. Energy Consumption Model

The energy consumption model [10] is based on the motion of the agent. The linear and angular velocities $\dot{p}_k$ and $\dot{\varphi}_k$ is the main variables in energy consumption model.

$$\dot{E}_k(t) = -k_e \beta_t \frac{{E_k}^2}{{E_{max}}^2} (\|\dot{p}_k\|^2 + \|\dot{\varphi}_k\|^2) \tag{17}$$

where $E_k(t) \in [0, E_{max}]$ is the capacity of embodied energy and $k_e > 0, \beta_t > 0$ are the model coefficients.

B. Power-Aware Control Laws

According to the energy consumption model (17), we propose the following power-aware coverage control laws which take the energy consumption of the mobile nodes into account. For the agents with single integrator dynamics, the control law is:

$$u_k = k_1 (p_k - C_{V_k}) - k_2 \left({\dot{p}_{k,x}}^2 + {\dot{p}_{k,y}}^2 \right) \tag{18}$$

where $k_1 > 0,\ k_2 > 0$ are the control gains.

For the non-holonomic agents, the control laws are given as in (19):

$$\begin{pmatrix} u_k \\ \omega_k \end{pmatrix} = \begin{pmatrix} (\gamma_1 cos\psi_k) e_k - (\gamma_2 cos\psi_k ({\dot{p}_{k,x}}^2 + {\dot{p}_{k,y}}^2)) e_k \\ 2(\gamma_1 - \gamma_2 ({\dot{p}_{k,x}}^2 + {\dot{p}_{k,y}}^2)) sin\psi_k cos\psi_k + \lambda_1 (\psi_k + \theta_k) \end{pmatrix} \tag{19}$$

where $\gamma_1 > 0,\ \gamma_2 > 0,\ \lambda_1 > 0$ are the control gains.

The stability analysis of the control law is given in the following section.

C. Repulsive Forces

Repulsive forces are used to prevent the robots from collision and the theory comes from the potential functions [16]. The definition of the potential functions is the addition of the attractive forces pulling the robot to the end configuration and the repulsive forces keeping the robot distant from other objects. The forces are defined as:

$$\vec{F}(q) = -\vec{\nabla} \mathrm{A}(q) \tag{20}$$

The potential function is defined as:

$$\mathrm{A}(q) = \mathrm{A}_{att}(q) + \mathrm{A}_{rep}(q) \tag{21}$$

The definition of the repulsive potential function is:

$$A_{rep}(q) = \begin{cases} \frac{1}{2}\zeta\left(\frac{1}{\rho(q)} - \frac{1}{\rho_0}\right)^2 & if\rho(q) \le \rho_0 \\ 0 & if\rho(q) > \rho_0 \end{cases} \quad (22)$$

where $\zeta > 0$ is a positive scaling factor, ρ_0 is distance of influence and $\rho(q)$ is the distance function from obstacle region CB to the agent. It is taken as:

$$\rho(q) = \min_{q' \in CB} \|q - q'\| \quad (23)$$

The repulsive force can be calculated as:

$$F_{rep}(q) = \begin{cases} \zeta\left(\frac{1}{\rho(q)} - \frac{1}{\rho_0}\right)\frac{1}{\rho^2(q)}\vec{\nabla}\rho(q) & if\rho(q) \le \rho_0 \\ 0 & if\rho(q) > \rho_0 \end{cases} \quad (24)$$

$$F_{rep,x}(q) = \|F_{rep}(q)\|\cos(\varphi_k - \vartheta) \quad (25)$$

$$F_{rep,y}(q) = \|F_{rep}(q)\|\sin(\varphi_k - \vartheta) \quad (26)$$

where ϑ is the angle between the obstacle and the robot. The repulsive force is then multiplied with a coefficient c and integrated once to obtain the velocity.

$$u_k' = \int cF_{rep,x}(q)dt \quad (27)$$

$$\omega_k' = \int cF_{rep,y}(q)dt \quad (28)$$

$$\overline{u_k} = u_k + u_k' \quad (29)$$

$$\overline{\omega_k} = \omega_k + \omega_k' \quad (30)$$

The final velocity formulation in (29) and (30) provides collision avoidance among the mobile agents.

VI. Stability Analysis

In this section, the Lyapunov stability analysis of the proposed controller will be given. We consider n non-holonomic agents with dynamics (11) and control laws (13)-(15) and (19). So, we start with defining m_k:

$$m_k = p_k - \hat{C}_{V_k} = -\begin{pmatrix} e_k\cos(\psi_k + \varphi_k) \\ e_k\sin(\psi_k + \varphi_k) \end{pmatrix} \quad (31)$$

We define the Lyapunov function candidate as follows:

$$V = \sum_k \begin{pmatrix} {m_k}^T K_1 m_k + {\tilde{\varsigma}_k}^T K_2 \tilde{\varsigma}_k + \\ \kappa_3(\psi_k + \theta_k)^2 + E_k(t) \end{pmatrix} \quad (32)$$

Here $K_1 \in \mathbb{R}^{2x2}$ and $K_2 \in \mathbb{R}^{mxm}$ denote positive definite matrices and κ_3 is a positive constant. Taking the derivative of the Lyapunov candidate yields:

$$\dot{V} = 2\sum_k \begin{pmatrix} {m_k}^T K_1 \dot{m}_k + {\tilde{\varsigma}_k}^T K_2 \dot{\tilde{\varsigma}}_k \\ +\kappa_3\begin{pmatrix} \psi_k\dot{\psi}_k + \psi_k\dot{\theta}_k \\ +\dot{\psi}_k\theta_k + \theta_k\dot{\theta}_k \end{pmatrix} \\ -k_e\beta_t\frac{{E_k}^2}{{E_{max}}^2}(\|\dot{p}_k\|^2 + \|\dot{\varphi}_k\|^2) \end{pmatrix} \quad (33)$$

If we replace (13) in ((29)) we get the derivative of the Lyapunov function as follows:

$$\dot{V} = 2\sum_k \begin{pmatrix} {m_k}^T K_1 \dot{m}_k \\ -{\tilde{\varsigma}_k}^T K_2 P Z^T Z \tilde{\varsigma}_k \\ -\eta{\tilde{\varsigma}_k}^T K_2 \sum_{l\in\mathcal{L}_k}(\hat{\varsigma}_l - \hat{\varsigma}_k) \\ +\kappa_3\begin{pmatrix} \psi_k\dot{\psi}_k + \psi_k\dot{\theta}_k \\ +\dot{\psi}_k\theta_k + \theta_k\dot{\theta}_k \end{pmatrix} \\ -k_e\beta_t\frac{{E_k}^2}{{E_{max}}^2}(\|\dot{p}_k\|^2 + \|\dot{\varphi}_k\|^2) \end{pmatrix} \quad (34)$$

The first term is negative. The proof is given in [1].

$$\dot{m}_k = -\begin{pmatrix} (\gamma_1 - \gamma_2({\dot{p}_{k,x}}^2 + {\dot{p}_{k,y}}^2))cos\psi_k e_k\cos(\psi_k + \varphi_k) \\ (\gamma_1 - \gamma_2({\dot{p}_{k,x}}^2 + {\dot{p}_{k,y}}^2))cos\psi_k e_k\sin(\psi_k + \varphi_k) \end{pmatrix} \quad (35)$$

where $\frac{\gamma_1}{\gamma_2} \ge \max({\dot{p}_{k,x}}^2 + {\dot{p}_{k,y}}^2)$.

$$\sum_k {m_k}^T K_1 \dot{m}_k = \\ -\sum_k(\gamma_1 - \gamma_2({\dot{p}_{k,x}}^2 + {\dot{p}_{k,y}}^2)){e_k}^2 cos^2\psi_k \le 0 \quad (36)$$

Since $P(t)$ is positive definite and converges to zero as given in [15], the second term gives:

$$-{\tilde{\varsigma}_k}^T K_2 P Z^T Z \tilde{\varsigma}_k \le 0 \quad (37)$$

For the third term, the proof is given as below. The detailed proof for the binary protocol is given in [17]. Here A_{kl} denotes the adjacency matrix.

$$-\eta\sum_k {\tilde{\varsigma}_k}^T \sum_{l\in\mathcal{L}_k}(\hat{\varsigma}_k - \hat{\varsigma}_l) \\ = -\frac{1}{2}\eta\sum_k\sum_{l\in\mathcal{L}_k} A_{kl}(\hat{\varsigma}_k - \hat{\varsigma}_l)^T(\hat{\varsigma}_k - \hat{\varsigma}_l) \\ \le -\frac{1}{2}\eta\sum_k\sum_{l\in\mathcal{L}_k}\|\hat{\varsigma}_k - \hat{\varsigma}_l\|^2 \quad (38)$$

The fourth term becomes:

$$\sum_k \kappa_3\begin{pmatrix} \psi_k\dot{\psi}_k + \psi_k\dot{\theta}_k \\ +\dot{\psi}_k\theta_k + \theta_k\dot{\theta}_k \end{pmatrix} \\ = \sum_k \kappa_3(\psi_k + \theta_k)\left(2u_k\frac{sin\psi_k}{e_k} - \omega_k\right) \\ = \sum_k \kappa_3\lambda_1(\psi_k + \theta_k)^2 \le 0 \quad (39)$$

The fifth term is negative since E_k, $\|\dot{p}_k\|$ and $\|\dot{\varphi}_k\|$ are positive.

$$-k_e\beta_t\frac{{E_k}^2}{{E_{max}}^2}(\|\dot{p}_k\|^2 + \|\dot{\varphi}_k\|^2) \le 0 \quad (40)$$

Since V is positive definite and lower bounded, $\dot{V} \le 0$ and $\ddot{V}$ is bounded, then by Barbalat's Lemma $e_k \to 0$, $|\psi_k| \to 0$, $|\theta_k| \to 0$, $\tilde{\varsigma}_k \to 0$ and $\|\hat{\varsigma}_l - \hat{\varsigma}_k\| \to 0$ as $t \to \infty$.

VII. Simulation Results

Simulations are carried out in MATLAB environment with 5 agents. The dimensions of the map are 10 by 10 meters.

The coefficients used in simulations are $\gamma_1 = 0.3$, $\gamma_2 = 0.4$, $\lambda_1 = 2.5$, $\lambda_f = 8.0$ and $\eta = 2$. For the repulsive fields, the gains are chosen as $\zeta = 10$, $\rho_0 = 0.5$ and $c = 1$.

The distributed density function $\phi(q)$ is chosen as expanding circle and it is triggered at certain times in the simulation. The estimated density function $\hat{\phi}_k(q)$ is divided into 64 cells. The vector function Z is chosen as:

$$\mathrm{Z}_k(q) = e^{\frac{-(q-\mu_k)^2}{2\sigma_k{}^2}} > 0 \qquad (41)$$

where $\sigma_k{}^2 = 0.05$. Z_k denotes k^{th} term of the vector function and μ_k is the center of the Gaussian function.

The results of the simulation carried out are given in figures 3-9. Figure 3 shows two simulation frames in which the position and orientation of mobile agents and corresponding density functions are given.

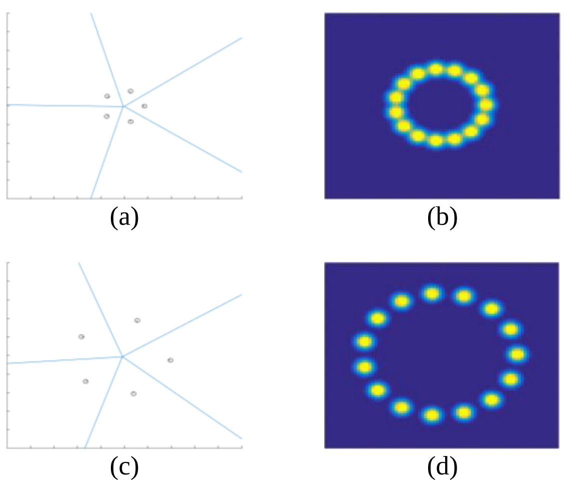

Figure 3. The positions and orientations of the mobile agents given in (a) and (c), and corresponding density functions given in (b) and (d)

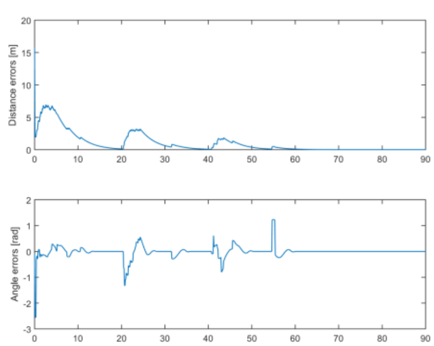

Figure 4. Distance and angular errors

In Figure 4, the distance and angular errors of 5 agents show that the multi-agent system with the proposed controller is asymptotically stable.

In Figure 5 and Figure 6, the parameters converge to the actual values with a linear consensus protocol. As given in the proof in stability analysis section, the errors are going to zero asymptotically as the time goes to infinity.

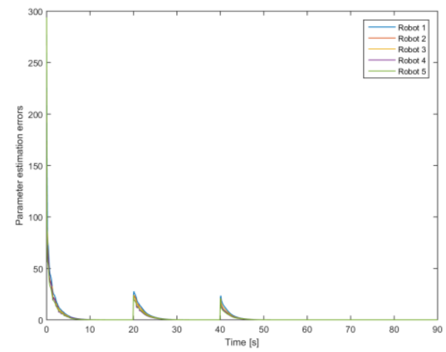

Figure 5. Parameter estimation errors

In Figure 6, the resulting errors of the linear consensus are given. The errors converge to zero as given in the result in the stability analysis section.

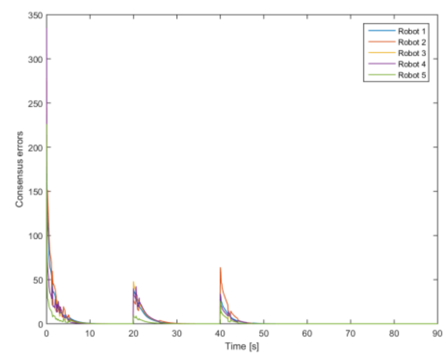

Figure 6. Consensus errors with linear consensus protocol

Figure 7 shows the effect of the power-aware control laws to the power consumption of the nodes for 5 agents. By changing the controller coefficients the total energy consumption of the nodes can be reduced. The result is verified with different coefficients.

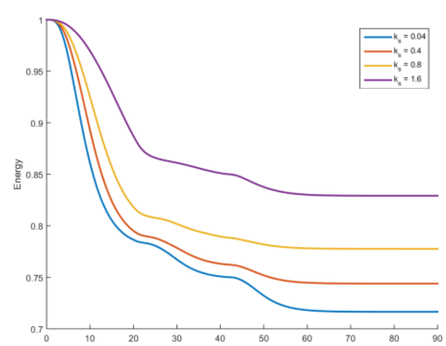

Figure 7. Energy consumption of the nodes with respect to controller parameters (5 agents)

In Figure 8, the simulation results with 10 agents show that the power consumption of the nodes are affected by changing the controller coefficients appropriately. By increasing the coefficient $\gamma_2 = k_s$, there is more energy left in the storage mediums.

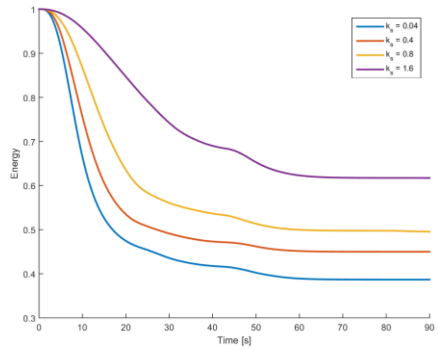

Figure 8. Energy consumption of the nodes with respect to controller parameters (10 agents)

In Figure 9, the simulation results with 15 agents are shown. By increasing the control coefficient γ_2, again, the power consumption is reduced.

VIII. CONCLUSIONS

In the paper, a new approach to the coverage control problem using adaptive coordination and power-aware control laws is proposed. The non-holonomic mobile agents estimate the dynamic density function and a linear consensus law are used.

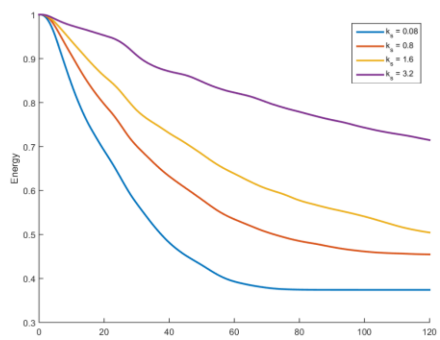

Figure 9. Energy consumption of the nodes with respect to controller parameters (15 agents)

A new adaptive power-aware controller is proposed and its stability analysis is given. According to the simulations carried out in MATLAB environment, the results show that with the used adaptive control laws, the mobile nodes estimate the density function. The estimation and consensus errors reach to zero asymptotically while the time goes to infinity.

By using the estimated density function, the mobile nodes position themselves by using the proposed power-aware control laws. Besides, the repulsive forces provide collision avoidance. Also, the simulation is carried out with 5, 10 and 15 agents. By changing the controller coefficients the total energy consumption of the mobile agents can be reduced. The theoretical results are verified with simulation results.

REFERENCES

[1] Luna, J. M., Fierro, R., Abdallah, C. T., & Lewis, F. L. "A binary consensus approach to decentralized coordination of nonholonomic sensor networks", *Proceedings of the IEEE Conference on Decision and Control*, 2012, pp. 3353-3359.
[2] A. Deshpande, S. Poduri, D. Rus, and G. S. Sukhatme, "Distributed coverage control for mobile sensors with location-dependent sensing models," *in Proc. of the Intl. Conf. on Robotics and Automation (ICRA 09)*, Kobe, Japan, May 2009, pp. 2344–2349.
[3] S. Martínez, T. Karatas, F. Bullo J. Cortés, "Coverage Control for Mobile Sensing Networks," *IEEE Transactions on Robotics and Automation*, vol. 20, no. 2, pp. 243-255, 2004.
[4] Fu, J. G. M., Bandyopadhyay, T., & Ang Jr, M. H., "Local Voronoi decomposition for multi-agent task allocation", *in IEEE International Conference on Robotics and Automation*, May 2009, pp. 1935-1940.
[5] A. Okabe and A. Suzuki, "Locational optimization problems solved through Voronoi diagrams," *Eur. J. Oper. Res*., vol. 98, no. 3, pp. 445-56, 1997.
[6] A. Howard, M. J. Mataric and G. S. Sukhatme, "Mobile sensor network deployment using potential fields : a distributed, scalable solution to the area coverage problem," *Proc. 6th Int. Symposium on Distributed Autonomous Robotics Systems*, pp. 299-308, 2002.
[7] W. Dunbar and R. Murray, "Distributed Receding Horizon control for Multi-Vehicle formation stabilization, " *Automatica*, vol. 42, no. 4, pp. 549-558, 2006.
[8] T. Hatanaka, M. Fujita A. Gusrialdi, "Coverage Control for Mobile Networks with Limited-Range Anisotropic Sensors", *in Proceedings of the 47th IEEE Conference on Decision and Control*, Cancun, Mexico, 2008.
[9] Li, W. and Cassandras, C., 2005. "Distributed cooperative coverage control of sensor networks", *Proceedings of the IEEE Conference on Decision and Control*, pp. 2542 – 2547.
[10] A. Gusrialdi, R. Dirza, T. Hatanaka, M. Fujita, "Improved distributed coverage control for robotic visual sensor network under limited energy storage", Int. J. Imaging Robot, vol. 10, no. 2, pp. 58-74, 2013.
[11] Kwok, A., & Martinez, S., 2007. "Energy-balancing cooperative strategies for sensor deployment". *Proceedings of the IEEE Conference on Decision and Control*, 2007, pp. 6136-6141.
[12] Kwok, A., & Martinez, S., 2008. "Deployment algorithms for a power-constrained mobile sensor network". *IEEE International Conference on Robotics and Automation*, 2008, pp. 140-145.
[13] N. Heo and P. K. Varshney, "Energy-efficient deployment of intelligent mobile sensor networks," *IEEE Transactions on Systems, Man and Cybernetics*, Part A, vol. 35, no. 1, pp. 78-92, January 2005
[14] M. Aicardi, G. Casalino, A. Bicchi, and A. Balestrino, "Closed loop steering and path following for unicycle-like vehicles: a simple lyapunov function based approach," *IEEE Robotics Automation Magazine*, vol. 2, no. 1, pp. 27–35, March 1995.
[15] J. J. E. Slotine and W. Li, *Applied Nonlinear Control*. Upper Saddle River, NJ 07458: Prentice Hall, 1991.
[16] Latombe, J. C., Robot motion planning. Norwell, MA 02061: Kluwer Academic Publishers, 1991.
[17] Chen, G. & Lewis, F. L., 2011. "Synchronizing Networked Lagrangian Systems". *Preprints of the 18th IFAC World Congress*, 2011, pp. 1225-1230.